

## Structure and Mechanical Properties of Blends of an Amorphous Polyamide and an Amorphous Copolyester

Ainhoa Granado, Lara Iturriza, Jose Ignacio Eguiazábal

Dpto. de Ciencia y Tecnología de Polímeros and POLYMAT, Universidad del País Vasco/Euskal Herriko Unibertsitatea UPV/EHU, P.O. Box 1072, 20080 San Sebastián, Spain  
Correspondence to: J. I. Eguiazábal (E-mail: josei.eguiazabal@ehu.es)

**ABSTRACT:** This article deals with the structure and mechanical properties of blends of an amorphous copolyester (PCTG) and an amorphous polyamide (aPA) which were directly prepared during the plasticization step of an injection molding process. The blends were composed by an almost pure aPA phase, and a PCTG-rich phase where some aPA subparticles are present. The morphology of the blends showed both rather fine dispersed particles and occasionally large particles with occluded subparticles. This complex morphology indicated a low interface tension attributed to the presence of some aPA in the PCTG-rich phase of the blends. The almost linear behavior of the modulus of elasticity was attributed to the constancy of the main structural characteristics upon blending and the equally linear ductility to the good adhesion level and the presence of thin and elongated morphologies. © 2014 Wiley Periodicals, Inc. *J. Appl. Polym. Sci.* **2014**, *131*, 40785.

**KEYWORDS:** amorphous; mechanical properties; morphology; blends; phase behavior

Received 13 January 2014; accepted 28 March 2014

DOI: 10.1002/app.40785

### INTRODUCTION

Intensive research has been carried out with a view to broadening the scope of applications for polymers. This research involved blending them and controlling blend structures to fix certain properties of the blends.<sup>1</sup> Among the very wide variety of polymer blends, those made up of polyesters and polyamides have been widely studied. This is because they show very useful thermal and mechanical properties, and because they can offset some shortcomings of the other component, such as the high water absorption level of polyamides or the low extensibility of polyesters.<sup>2</sup>

The crystalline nature of the blend components usually gives rise to poor interphase properties in the solid state.<sup>3</sup> Moreover, when compared with semicrystalline polyamides, amorphous polyamides (aPAs) with their very variable chemical nature, show better optical properties and dimensional stability, lower water absorption and higher barrier properties to gases and solvents in wet environments.<sup>4,5</sup> These advantages make aPAs commercially attractive and have led to the study of the behavior when blended with many second components. Thus, blends of aPAs with polyesters,<sup>6–11</sup> PA6,<sup>12</sup> polyolefins,<sup>13–15</sup> ethylene-vinyl alcohol copolymer (EVOH),<sup>16–18</sup> poly(ether imide) (PEI),<sup>19</sup> acrylonitrile-styrene copolymer (SAN),<sup>20</sup> and poly(amino ether) resin (PAE)<sup>4</sup> have been studied. Recently, binary<sup>21</sup> and ternary<sup>22</sup> nanocomposites of aPAs, mainly with elastomers,<sup>23–25</sup> have also

been studied. The blends of aPAs with PA6 were miscible<sup>12</sup> while those with PEI and PAE were compatible.<sup>4,19</sup> However with polyolefins,<sup>15</sup> EVOH<sup>17</sup> and SAN<sup>20,26</sup> compatibilizers are required to obtain a minimum compatibility. Finally, blends of aPAs with polyesters have been studied the most; their miscibility level depends on the structure of the polyamide. Thus, while an amorphous copolyester (PETG), poly(ethylene terephthalate) (PET) and poly(butylene terephthalate) (PBT) show a single  $T_g$  when blended with Trogamid (a commercial aPA), indicating miscibility,<sup>6</sup> blends of PETG with Durethan T40 were immiscible.<sup>8</sup>

Among the aPAs, Selar<sup>®</sup> PA 3426 has one aromatic unit for every two amide groups, which changes the polarity and molecular volume per amide unit with respect to other polyamides. It is the most polar of the best known aPAs.<sup>27</sup> It exhibits excellent transparency, good barrier properties to gases, water, solvents and essential oils, and high temperature structural properties which make it suitable for a number of packaging applications.<sup>5</sup> With respect to its blends, those with an aromatic and crystalline polyamide<sup>28</sup> were completely immiscible, but transreaction was fast and produced a homogeneous system. Blends with crystalline PA6<sup>12</sup> may give rise to domains of nanometer scale. In the case of Selar/ethylene-propylene copolymer blends,<sup>14</sup> the effect of a grafted ethylene-propylene copolymer compatibilizer on the morphology and the impact strength were studied.

A fine morphology and immiscibility were found in Selar/SAN blends.<sup>20,26</sup> In the case of Selar/EVOH blends,<sup>29,30</sup> barrier properties were reported. However, the mechanical properties of Selar blends have hardly been studied in the literature.

Poly(ethylene glycol-co-cyclohexane-1,4 dimethanol terephthalate) (PCTG) is a transparent and tough amorphous copolyester used mainly for blister packaging, bags, cosmetic and fragrance caps, displays and refrigerator interior components.<sup>31</sup> Blends of PCTG with polycarbonate (PC),<sup>32</sup> PEI,<sup>33</sup> PAE<sup>34</sup> as well as nanocomposites of PCTG with an organically modified clay<sup>35</sup> have been studied recently. No blend with polyamides has been published to our knowledge. The blends of PCTG with PC were miscible.<sup>32</sup> The addition of low PCTG contents clearly increased the processability of PEI and led to almost linear mechanical properties with the composition in spite of the biphasic nature of the blends.<sup>33</sup> In the case of PAE/PCTG blends, the small dispersed phase size and good adhesion in spite of their immiscibility, also led to linear mechanical properties.<sup>34</sup> Thus, blends of PCTG with different kinds of polymers are attractive.

Surprisingly, PCTG/aPA blends have not been studied. For this reason, in this article the miscibility level of the PCTG/Selar blends was analyzed by differential scanning calorimetry (DSC) and dynamic mechanical analysis (DMA), the morphology by scanning electron microscopy (SEM), and the mechanical properties were determined by means of tensile tests.

## EXPERIMENTAL

The polymers used in this work were commercial products. The aPA (Selar<sup>®</sup> PA 3426, Du Pont) is a condensation product of hexamethylene diamine and a mixture of terephthalic/isophthalic acids, with a melt flow index (MFI) of  $4.9 \pm 0.2$  g  $10 \text{ min}^{-1}$ .<sup>36</sup> The amorphous copolyester (PCTG), Eastar PCTG DN011 from Eastman, is obtained by reacting terephthalic acid, 1,4-cyclohexane dimethanol and ethylene glycol with a 3:2:1 molar ratio.<sup>35</sup> It has an inherent viscosity of  $0.73 \text{ dL g}^{-1}$ . In order to prevent moisture-induced degradation reactions, both polymers were dried before processing in an air circulation oven, the aPA for 20 h at  $100^\circ\text{C}$  and the PCTG for 6 h at  $65^\circ\text{C}$ .

The PCTG/aPA blends with 15, 30, 50, 70 and 85% aPA contents were prepared by direct injection molding. A Battenfeld BA 230E reciprocating screw injection molding machine was used to obtain tensile (ASTM D-638, type IV) and impact (ASTM D-256) specimens. The screw had a diameter of 18 mm,  $L/D$  ratio of 17.8, compression ratio of 4, and helix angle of  $17.8^\circ$ . All compositions were processed at a melt temperature of  $230^\circ\text{C}$ . The mold temperature was  $15^\circ\text{C}$  and the injection speed and pressure were  $11.4 \text{ cm}^3 \text{ s}^{-1}$  and 2740 bar, respectively. The neat components were processed in the same way.

The phase behavior of the blends was analyzed by differential scanning calorimetry (DSC) and dynamic mechanical analysis (DMA). The DSC scans were carried out in a Perkin-Elmer DSC-7 calorimeter under a nitrogen atmosphere. The samples were first heated from 30 to  $175^\circ\text{C}$  at  $20^\circ\text{C min}^{-1}$  to erase any previous thermal history, then cooled to  $30^\circ\text{C}$  at the maximum speed provided by the calorimeter, and subsequently reheated as in the first scan. The glass transition temperatures ( $T_g$ ) were

determined from the second heating scans. The dynamic mechanical tests were carried out in a TA Instruments DMA Q800, in the flexural mode, at a frequency of 1 Hz and a heating rate of  $4^\circ\text{C min}^{-1}$  from 0 to  $175^\circ\text{C}$ . The  $T_g$ 's were determined from the peaks of the  $\tan \delta$ -temperature plots.

The possible reactions during processing were analyzed by Fourier transform infrared (FTIR) spectroscopy (Nicolet Magna IR 560 spectrometer). The FTIR spectra were obtained on the surfaces of tensile specimens. Density measurements were carried out in a Mirage SD-120L electronic densitometer with *n*-butyl alcohol as the immersion liquid. The temperature was controlled with a precision of  $\pm 0.1^\circ\text{C}$ . The orientation of the blends was measured using a Mettler Model 2010 equipped with an infrared laser with a wavelength of 1550 nm. The samples were prepared by sectioning the central part of the injected tensile specimens with a Leica 1600 microtome. Vicat softening temperatures were measured with an ATS Faar MP3 HDT-Vicat tester, at  $50^\circ\text{C h}^{-1}$  and with a 1000 g load (ASTM D-1525), using impact specimens.

Tensile tests were carried out on the injection-molded specimens with an Instron 5569 machine at a crosshead speed of  $10 \text{ mm min}^{-1}$ . The mechanical properties (yield stress and ductility, measured as the break strain) were determined from the load-displacement curves. Young's modulus was determined by means of an extensometer at a crosshead speed of  $1 \text{ mm min}^{-1}$ . A minimum of eight tensile specimens were tested for each reported value.

The surfaces of cryogenically fractured tensile specimens were observed by SEM after gold coating. A Hitachi S-2700 electron microscope was used at an accelerating voltage of 15 kV.

## RESULTS AND DISCUSSION

### Phase Behavior

Table I shows the  $T_g$ 's of the blends measured by both DSC and DMA with those of the neat PCTG and aPA as a reference. A similar trend was observed in both sets of values; as usual,<sup>37-39</sup> the  $T_g$  values of DMA were higher than those by DSC due to the mechanical dynamic nature of the test.<sup>40</sup> Two nearly constant  $T_g$ 's were observed by DSC whatever the blend composition, suggesting the presence of two almost neat amorphous phases. The  $T_g$  of the aPA determined by DMA also remained constant, within the experimental error. With respect to the low  $T_g$  values, corresponding to a PCTG-rich phase, only those of the PCTG/aPA 85/15 and 70/30 blends are shown. This is due to the decrease in the intensity of the corresponding  $\tan \delta$  peak and the simultaneous increase in the intensity of a shoulder that appeared at around  $103^\circ\text{C}$  (Figure 1) hindering the determination of  $T_g$ . As can also be seen in Figure 1 where the  $\tan \delta$ -temperature plots of the blends from DMA analysis are shown, this shoulder can be observed in most compositions of the blends. This may be related to the presence of small amounts of aPA mixed in the PCTG-rich phase. This is not reflected in the DSC data since the DMA technique is more sensitive than the DSC analysis in the detection of small transitions and disturbances caused by chemical interactions and/or reactions.<sup>41</sup> Moreover, in the DMA analysis (Figure 1), there was a

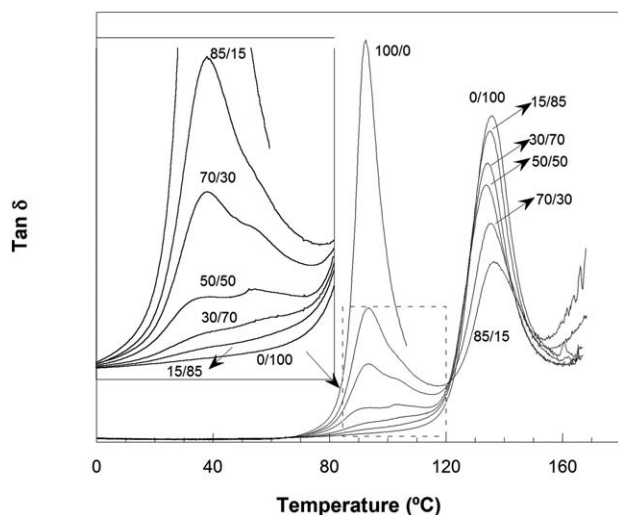


Figure 1.  $\tan \delta$  Scans of the PCTG/aPA blends measured by DMA.

noticeable widening of the  $T_g$  peak of PCTG in the blends. The width of the  $\tan \delta$  peaks, measured at the half height, is also shown on Table I. The increase in the width of the low temperature peak indicated compositional heterogeneity and contrasts with the almost constant width of the high temperature peak. These results indicate that PCTG/aPA blends are partially miscible and are made up of a practically pure aPA phase and a PCTG-rich phase containing small amounts of aPA.

A previous study<sup>42</sup> concerning the miscibility of polyamides with polyesters concluded that miscibility appeared to depend primarily upon the chemical composition of the constituents. Thus, while unfavorable thermodynamic interactions between both kinds of polymers causing immiscibility were expected in most systems, at least partial miscibility may appear in cases where the ratio between functional groups is favorable enough to overcome or at least partially compensate for these unfavorable interactions. In this way,<sup>42</sup> as the methylene content of both the polyamides and polyesters increases, the Flory–Huggins interaction parameter decreases, showing greater interaction. It has also been suggested<sup>6</sup> that the presence of identical aromatic moieties in the two polymers could also facilitate favorable interactions. This could explain the miscibility of the blends of Trogamid with PET, PETG and PBT.<sup>6</sup> In our case, while the

aromatic and cyclohexane rings of aPA and PCTG, respectively, could hinder miscibility, it would appear that the six methylene groups of the aPA and the possible interaction through hydrogen bonding between the hydrogen of the amide group of aPA and the oxygen of the carbonyl group of PCTG are responsible for the interaction between the two polymers.

### Morphology

The morphology of the cryogenically fractured surfaces of the tensile specimens observed by scanning electron microscopy (SEM) is shown in Figure 2. As can be seen, the blends are clearly multiphase with homogeneously distributed particles. Surprisingly, the photographs, with higher magnification in Figure 3, show that some of the dispersed particles, mostly in intermediate compositions and in the aPA-rich blends, contain inclusions of an obvious matrix nature. The high number of subparticles in the aPA-rich blends may be related to the viscosity of the materials, since the less viscous phase (in our case PCTG) tends to encapsulate the other phase, as this reduces the rate of energy dissipation.<sup>43,44</sup> The average dispersed particle size was slightly smaller in the PCTG-rich blends (when measured in the 70/30 and 30/70 compositions it was 0.18  $\mu\text{m}$  versus 0.33  $\mu\text{m}$ , respectively). The existence of subparticles<sup>4,28,45,46</sup> and the small particle size indicate a good mixing level which is especially relevant in the direct injection molding mixing procedure. This also means there is good interface contact indicating low interfacial tension between the components which is consistent with the proposed presence of some aPA in the PCTG-rich phase of all the blends.

In Figures 2(a,b) and 3(a), most particles appear broken instead of debonded, indicating that they were strongly anchored to the matrix; this indicates low interfacial tension in the melt state leading to good adhesion in the solid state. In the aPA-rich blends of Figures 2(d,e) and 3(b), however, debonding occurs much more often than in Figure 2(a,b) as seen by the protuberant (pulled out) elongated particles and the increased number of holes left in the matrix. This is probably because the particles in these compositions are longer and thicker.

The 50/50 blend [Figure 2(c)] showed a rather co-continuous morphology similar to that typical of the phase inversion region. This is because the morphology of the upper and lower parts in Figure 2(c) is close to that of Figure 2(a,b), and that of the centre close to the one shown in Figure 2(d,e). To ascertain

Table I. Glass Transition Temperatures ( $T_g$ , °C) and Widths at the Half Height of the  $\tan \delta$  peaks (°C), of PCTG/aPA Blends

PCTG/aPA	DSC		DMA			
	$T_g$ PCTG	$T_g$ aPA	$T_g$ PCTG	Width	$T_g$ aPA	Width
100/0	87		93	8		
85/15	87	124	93	13	136	16
70/30	88	124	93	16	135	15
50/50	88	123	–	20	134	15
30/70	89	125	–	17	134	14
15/85	88	124	–	–	135	14
0/100	–	125	–	–	136	14

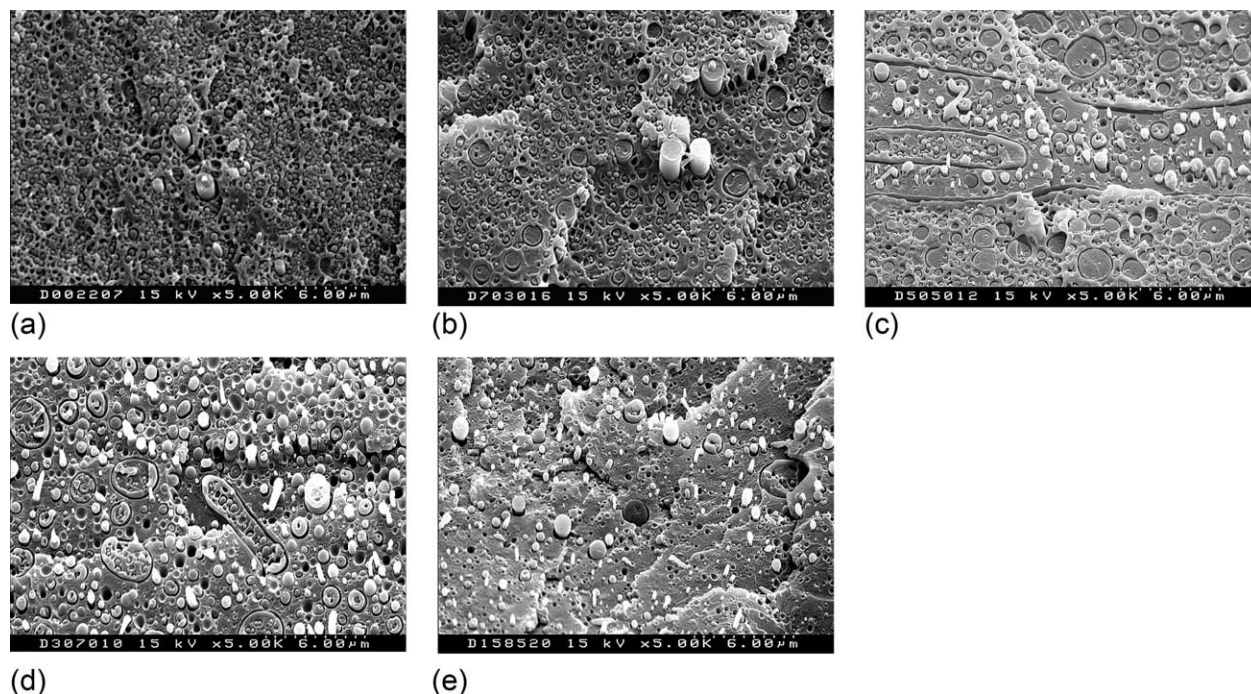


**Figure 2.** SEM photomicrographs of the surfaces of cryogenically fractured PCTG/aPA 85/15 (a), 70/30 (b), 50/50 (c), 30/70 (d), and 15/85 (e) blends.

the nature of the matrix in Figure 2(c), the phase inversion composition was estimated by the Vicat softening temperature-composition plot for the blends (Figure 4).<sup>47</sup> The Vicat temper-

ature of the 50/50 blend was close to that of the neat aPA, indicating the aPA-rich nature of the matrix.

Finally, a large contact area obtained through an elongated dispersed phase,<sup>44,48–50</sup> the presence of subparticles, and good interphase adhesion,<sup>34,45,46</sup> are all parameters that would point towards positive mechanical behavior in these biphasic blends studied in the following section.

### Mechanical Properties

Young's modulus and the yield stress of the blends are plotted versus composition in Figure 5. The solid and dashed lines correspond to the linear interpolation between the values of the neat polymers and are used as a reference to determine the

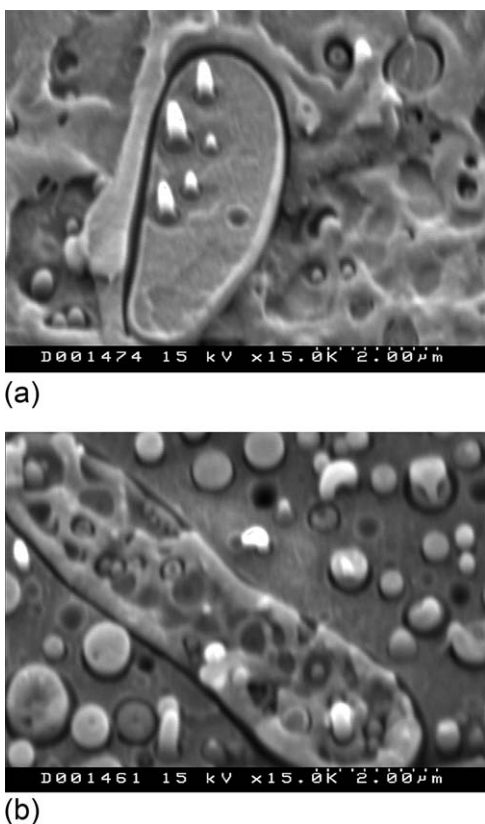


**Figure 3.** SEM photomicrographs of the surfaces of cryogenically fractured PCTG/aPA 70/30 (a) and 30/70 (b) PCTG/aPA blends at high magnification.

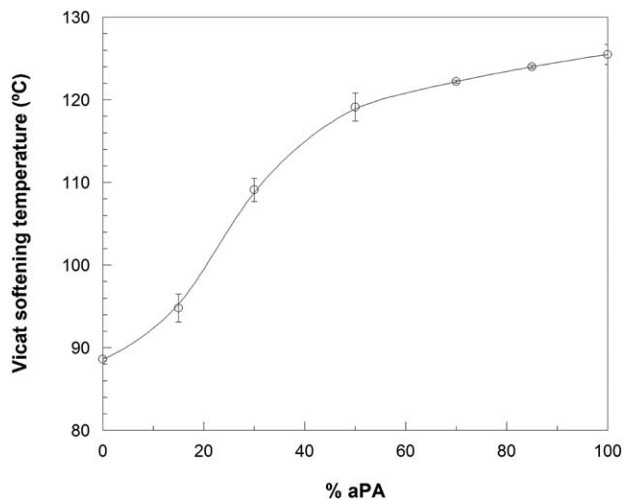


**Figure 4.** Vicat softening temperature of PCTG/aPA blends as a function of composition.

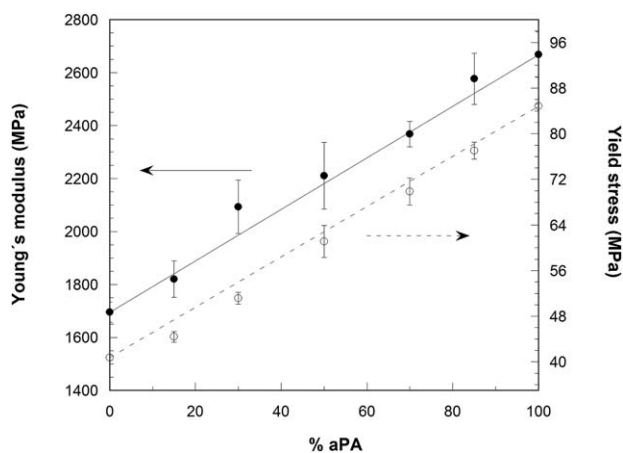


**Figure 5.** Young's modulus (●) and yield stress (○) of PCTG/aPA blends as a function of composition.

changes produced by mixing. As it is seen, both properties changed almost linearly with the composition. The similar behavior of both properties is common in polymer blends.<sup>51</sup> Linear or quasilinear behavior of the modulus of elasticity is often seen in miscible blends.<sup>52</sup> It can also appear in immiscible systems,<sup>53–55</sup> where interactions and interface adhesion are supposed to be weak. This is because low adhesion should be enough to assure cohesion and stress transmission at the low strain levels where the modulus is measured.

Changes in the free volume and/or a different orientation of the components in the blends and in the neat state may cause this modulus behavior. It was unlikely that any interchange reaction took place during processing because interchange reactions between polyesters and polyamides are very slight,<sup>53,56,57</sup> and must be initiated by a catalyst.<sup>58,59</sup> Moreover, the processing time in this study was very short (less than 1 min) compared to previous studies where the interchange reactions took place

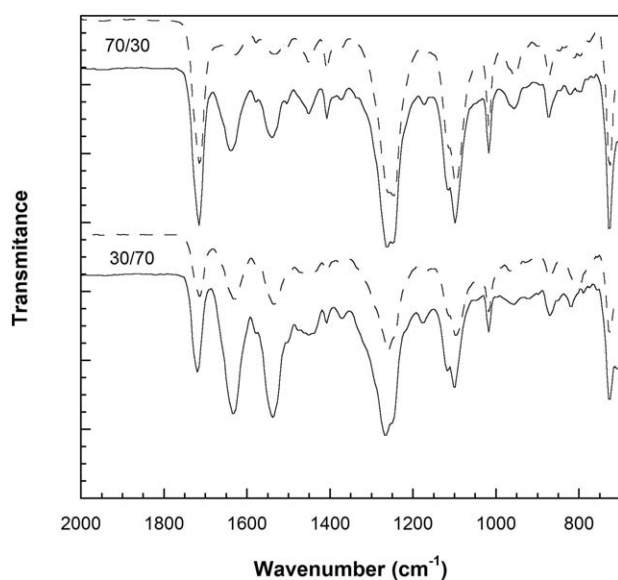


**Figure 6.** Experimental (solid lines) and calculated (dashed lines) FTIR spectra for the 70/30 and 30/70 PCTG/aPA blends.

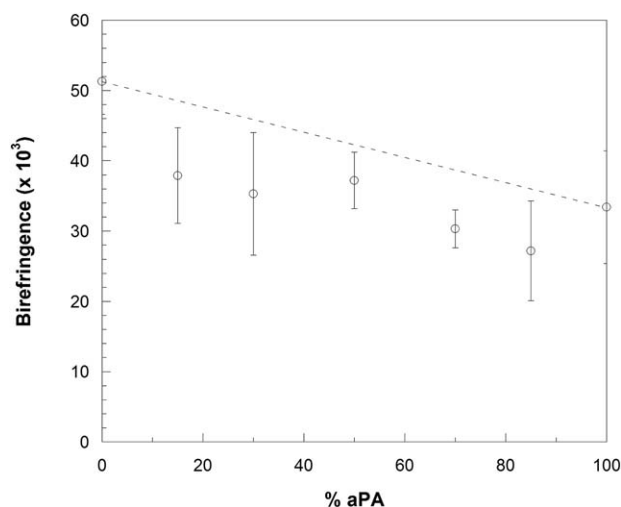


**Figure 7.** Birefringence of the PCTG/aPA blends as a function of composition.

effectively (more than 10 min in blends without catalysis<sup>56</sup> and 2–4 min in the case of catalyzed blends<sup>59</sup>). However, an additional test concerning interchange reactions was made by FTIR (Figure 6) comparing the experimental spectra of PCTG/aPA 70/30 and 30/70 blends, with those calculated by weighted addition of the spectra of the neat components. As observed in Figure 6, both spectra are very similar, so any reactions, if they did occur, were negligible. This indicates the presence of small amounts of unreacted aPA in the PCTG-rich phase of the blends. The plot of the specific volume of the blends against composition was linear, indicating that the free volume did not change upon mixing. Figure 7 shows the birefringence values of the blends against composition. The slight negative deviation from the linearity, which is taken as a reference, indicated that the molecular orientation was similar in the blends and in the neat components. Therefore, it can be concluded that the linear modulus is the result of no change in the main morphological characteristics of the components upon blending.

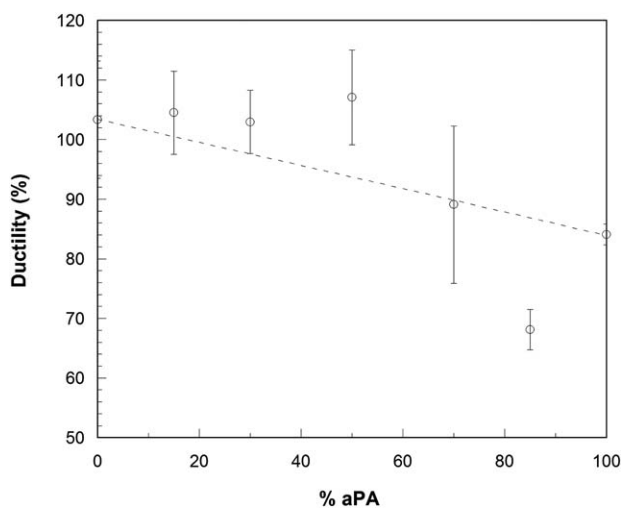


**Figure 8.** Ductility of the PCTG/aPA blends as a function of composition.

The break strain data are shown in Figure 8. Both the blends and the neat components were ductile and broken during the cold drawing stage of the deformation. This means that the differences observed are too small to be considered significant from a structural point of view. This positive ductility behavior is not typical of immiscible blends and is attributed to both the slight presence of some aPA in the PCTG phase of the blends and to the quite thin and elongated dispersed morphology of the blends which is known to often lead to ductile responses.<sup>45,49,60</sup>

## CONCLUSIONS

Directly injection-molded PCTG/aPA blends were partially miscible. Although the blends showed two nearly constant  $T_g$ 's by DSC, a shoulder was observed by DMA in the high temperature side of the  $T_g$  peak of PCTG. This indicated that the blends were made up of an almost pure aPA phase and a PCTG-rich phase where slight amounts of aPA were present.

Despite the absence of a previous mixing stage, direct injection molding was effective. This was deduced from both the small dispersed particle size (typically around 0.3  $\mu\text{m}$ ) and the existence of subparticles within the dispersed phase. This also reflected low interfacial tension in the melt state, and consequently, significant adhesion in the solid state.

The modulus of elasticity and the yield stress of the blends showed additive values resulting from the constancy of orientation and free volume upon blending. The positive ductility behavior was attributed to both the slight presence of some aPA in the PCTG phase of the blends, and the rather thin and elongated morphology of the blends which is known to often give rise to ductile responses.

## ACKNOWLEDGMENTS

The financial support of the Basque Government (Project no. IT611-13) and the University of the Basque Country (UFI11/56) is gratefully acknowledged.

## REFERENCES

1. Paul, D. R.; Bucknall, C. B. *Polymer Blends*; Wiley Interscience: New York, **2000**.
2. Utracki, L. A. *Commercial Polymer Blends*; Chapman & Hall: London, **1998**.
3. Kamal, M. R.; Sahto, M. A.; Utracki, L. A. *Polym. Eng. Sci.* **1982**, *22*, 1127.
4. Granado, A.; Eguiazábal, J. I.; Nazábal, J. *Macromol. Mat. Eng.* **2004**, *289*, 281.
5. Technical information from Pont.
6. Nadkarni, V. M.; Shingankuli, V. L.; Jog, J. P. *Polym. Eng. Sci.* **1988**, *28*, 1326.
7. García, M.; Eguiazábal, J. I.; Nazábal, J. *Polym. Compos.* **2003**, *24*, 555.
8. Gemeinhardt, G. C.; Moore, A. A.; Moore, R. B. *Polym. Eng. Sci.* **2004**, *44*, 1721.
9. Gemeinhardt, G. C.; Moore, R. B. *Macromolecules* **2005**, *38*, 2813.
10. Jang, S. H.; Kim, B. S. *Polym. Eng. Sci.* **1994**, *34*, 847.
11. García, M.; Eguiazábal, J. I.; Nazábal, J. *Polym. Compos.* **2003**, *24*, 555.
12. Cao, K.; Li, Y.; Yao, Z.; Zhou, G.-D.; Zeng, C.; Huang, Z.-M. *J. Appl. Polym. Sci.* **2012**, *124*, 1447.
13. Chen, J. C.; Harrison, I. R. *Polym. Eng. Sci.* **1998**, *38*, 371.
14. Kim, J. K.; Park, S. H.; O, H. T.; Jeon, H. K. *Polymer* **2001**, *42*, 2209.
15. Aramburu, N.; Eguiazábal, J. I. *J. Appl. Polym. Sci.* **2013**, *127*, 5007.
16. Lagarón, J. M.; Giménez, E.; Saura, J. J.; Gavara, R. *Polymer* **2001**, *42*, 7381.
17. Giménez, E.; Suay, J.; Arnau, G.; Saura, J.; Habib, K. A. *App. Mech. Eng.* **1999**, 207.
18. Lagarón, J. M.; Giménez, E.; Gavara, R.; Saura, J. J. *Polymer* **2001**, *42*, 9531.
19. Ramiro, J.; Eguiazábal, J. I.; Nazábal, J. *Eur. Polym. J.* **2006**, *42*, 458.
20. Becker, D.; Hage, E.; Pessan, L. A. *J. Appl. Polym. Sci.* **2010**, *115*, 2540.
21. Goitisoló, I.; Eguiazábal, J. I.; Nazábal, J. *Polym. Adv. Tech.* **2009**, *20*, 1060.
22. Goitisoló, I.; Eguiazábal, J. I.; Nazábal, J. *Macromol. Mater. Eng.* **2010**, *295*, 233.
23. González, I.; Eguiazábal, J. I.; Nazábal, J. *Polym. J.* **2012**, *44*, 294.
24. Yoo, Y.; Tiwari, R. R.; Yoo, Y.-T.; Paul, D. R. *Polymer* **2010**, *51*, 4907.
25. Yoo, Y.; Paul, D. R. *Ann. Tech. Confer.-Soc. Plast. Eng.* **2009**, *67*, 460.
26. Becker, D.; Porcel, F.; Hage, E.; Pessan, L. A. *Polym. Bull.* **2008**, *61*, 353.
27. Ellis, T. S. *Macromolecules* **1991**, *24*, 3845.
28. Ellis, T. S. *Polymer* **1995**, *36*, 3919.
29. Schell, T. A.; Paterka, M. C. **2006**, WO2006/063208.
30. Ofstein, D. E. **1991**, US5003002.
31. Technical information from Eastman.
32. Hopson, P. L.; Moore, R. B. *Mater. Res. Soc. Symp. Proc.* **2005**, 856E.
33. Granado, A.; Eguiazábal, J. I.; Nazábal, J. *Macromol. Mat. Eng.* **2010**, *295*, 476.
34. Granado, A.; Eguiazábal, J. I.; Nazábal, J. *Macromol. Mat. Eng.* **2006**, *291*, 1074.
35. Gonzalez, I.; Eguiazábal, J. I.; Nazábal, J. *Macromol. Mat. Eng.* **2008**, *293*, 781.
36. Becker, D.; Hage, E.; Pessan, L. A. *J. Appl. Polym. Sci.* **2007**, *106*, 3248.
37. Lampman, S. *Characterization and Failure Analysis of Plastics*; ASM International: USA, **2003**.
38. Madhukar, K.; Sainath, A. V. S.; Bikshamaiah, N.; Srinivas, Y.; Babu, N. M.; Ashok, B.; Kumar, D. S.; Rao, B. S. *J. Therm. Anal. Calorim.* **2014**, *115*, 345.

39. Backfolk, K.; Holmes, R.; Ihalainen, P.; Sirviö, P.; Triantafillopoulos, N.; Peltonen, J. *Polym. Test.* **2007**, *26*, 1031.
40. Martin, D. J.; Meijs, G. F.; Renwick, G. M.; Gunatillake, P. A.; McCarthy, S. J. *J. Appl. Polym. Sci.* **1996**, *60*, 557.
41. Da Costa, S. C. G.; Felisberti, M. I. *J. Appl. Polym. Sci.* **1999**, *72*, 1835.
42. Ellis, T. S. *Polymer* **1997**, *38*, 3837.
43. Barlow, J. W.; Paul, D. R. *Polym. Eng. Sci.* **1981**, *21*, 985.
44. Paul, D. R.; Barlow, J. W. *J. Macromol. Sci., Rev. Macromol. Chem.* **1980**, *C18(1)*, 109.
45. Granado, A.; Eguiazábal, J. I.; Nazábal, J. *J. Appl. Polym. Sci.* **2011**, *121*, 161.
46. Granado, A.; Eguiazábal, J. I.; Nazábal, J. *J. Appl. Polym. Sci.* **2008**, *109*, 3892.
47. Bastida, S.; Eguiazábal, J. I.; Nazábal, J. *Polym. Test.* **1993**, *12*, 233.
48. Zoldan, J.; Siegmann, A.; Narkis, M. *J. Macromol. Sci.-Phys.* **2005**, *B44*, 495.
49. Eguiazábal, J. I.; Nazábal, J. *Plast. Rubb. Process. Appl.* **1990**, *14*, 211.
50. Li, Z. M.; Xie, B. H.; Yang, S. Y.; Huang, R.; Yang, M. B. *J. Mat. Sci.* **2004**, *39*, 433.
51. Brown, N., *Failure of Plastics*; Hanser Publishers: Munich, **1986**.
52. Erro, R.; Gaztelumendi, M.; Nazábal, J. *New Polym. Mater.* **1992**, *3*, 87.
53. Retolaza, A.; Eguiazábal, J. I.; Nazábal, J. *Polym. Eng. Sci.* **2004**, *44*, 1405.
54. Kang, T. K.; Kim, Y.; Cho, W. J.; Ha, C. S. *Polym. Eng. Sci.* **1996**, *36*, 2525.
55. Arzak, A.; Eguiazábal, J. I.; Nazábal, J. *J. Appl. Polym. Sci.* **1995**, *58*, 653.
56. Chiu, F. C.; Lee, H. Y.; Wang, Y. H. *J. Appl. Polym. Sci.* **2008**, *107*, 3831.
57. Serhatkulu, T.; Erman, B.; Bahar, I.; Fakirov, S.; Evstatiev, M.; Sapundjieva, D. *Polymer* **1995**, *36*, 2371.
58. Pillon, L. Z.; Lara, J.; Pillon, D. W. *Polym. Eng. Sci.* **1987**, *27*, 984.
59. Pillon, L. Z.; Utracki, L. A. *Polym. Eng. Sci.* **1984**, *24*, 1300.
60. Guerrica-Echevarría, G.; Eguiazábal, J. I.; Nazábal, J. *J. Appl. Polym. Sci.* **1999**, *72*, 1113.